Extended Abstracts of the 21st Conference on Solid State Devices and Materials, Tokyo, 1989, pp. 449-452

GaAs/AlGaAs Double-Heterojunction Bipolar Transistor Carrier-Injected Optical Intensity Modulator

Y. Okada, K. Tada, R. J. Simes*, L. A. Coldren*, and J. L. Merz*

Department of Electronic Engineering, University of Tokyo,
7-3-1 Hongo, Bunkyo-ku, Tokyo, Japan.

**Department of Electrical and Computer Engineering,*
University of California, Santa Barbara, California 93106, U.S.A.

In this work, basic experimental results obtained with a GaAs/AlGaAs double-heterojunction bipolar transistor (DHBT) single-waveguide structure carrier-injected optical intensity modulator are presented and discussed for the first time. The output light intensity varied almost linearly with carrier injection mainly due to the carrier-induced band-filling and plasma dispersion effects, and up to 43% optical modulation has been obtained at a pulsed emitter current of 100 mA. Transistor characteristics has also been measured and analyzed.

1. Introduction

Optical modulators and switches with small device sizes, high on/off ratios and high speeds are expected to play very important roles in such areas as optical communications, optical signal processing, and optoelectronic or photonic integrated circuits (OEIC's or PIC's). Recently, in addition to the developments of the more widely-studied types of devices that utilize the field-induced effects in reverse-biased multiple quantum well (MQW) waveguide structures[1], optical modulators and switches that are operated by various carrier-induced effects have gained much interest and have been demonstrated with simple *p-i-n* double-heterostructure (DH) structures in InP/InGaAsP [2] as well as with GaAs/AlGaAs MQW structures [3], [4].

We have proposed and analyzed the first double-heterojunction bipolar transistor (DHBT) waveguide structure carrier-injected optical modulator/ switch, and have shown that the overall performance of the carrier-injected devices, particularly the modulation/switching speeds, can be improved significantly with this device configuration [5], [6].

In this work, device fabrication and some basic experimental results obtained with a GaAs/AlGaAs DHBT single-waveguide structure carrier-injected optical intensity modulator grown by molecular beam epitaxy (MBE) are presented for the first time.

2. Device Fabrication

The device fabrication starts with an epitaxial growth of the following five layers in sequence on an (100)-oriented n^+-GaAs (Si-doped to 1×10^{18} cm^{-3}) substrate by MBE; 1.0 μm-thick n^+-GaAs buffer layer (Si-doped to 1×10^{18} cm^{-3}), 1.0 μm-thick N-Al$_{0.2}$Ga$_{0.8}$As collector (cladding) layer (Si-doped to 1×10^{17} cm^{-3}), 0.3 μm-thick p^+-GaAs base (waveguide) layer (Be-doped to 1×10^{18} cm^{-3}, λ_g= 880 nm), 0.5 μm-thick N-Al$_{0.2}$Ga$_{0.8}$As emitter (cladding) layer (Si-doped to 5×10^{17} cm^{-3}), and finally, 0.3 μm-thick n^+-GaAs cap layer (Si-doped to 1×10^{18} cm^{-3}). The emitter-mesa or stripe-waveguide configuration of typically 7 μm in width, and the base-mesa of 50 μm in width were both defined using a H_3PO_4:H_2O_2:H_2O = 4:1:50 wet-etch. After sputtering a 2000Å-thick SiO_2 insulation layer, the emitter contact area was opened using a buffered HF and Ni/AuGe/Au contact metallization was evaporated and lifted off. An n-type

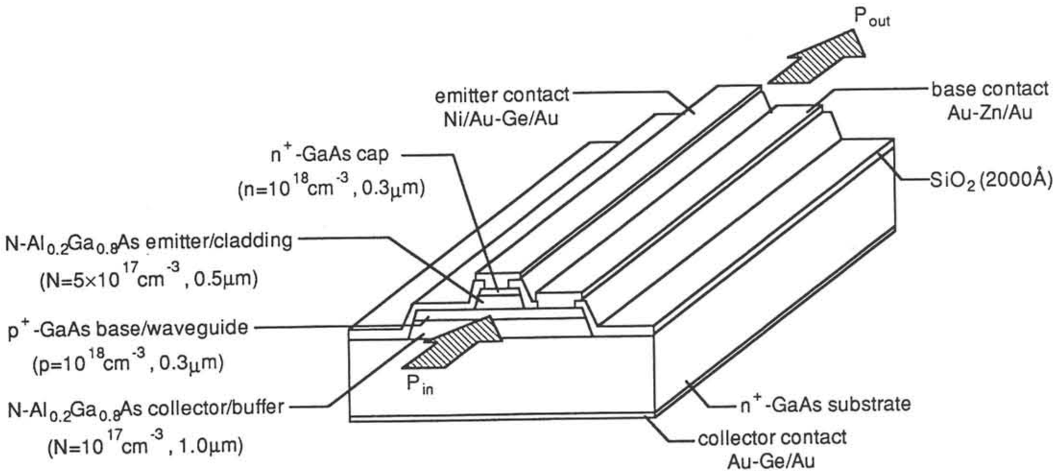

Fig. 1 A schematic structure of the DHBT carrier-injected optical intensity modulator.

ohmic contact to the emitter was then obtained by alloying the wafer in a flowing N_2 atmosphere at 430 °C for 45 sec. For *p*-type ohmic contact to the base, AuZn/Au was evaporated and was alloyed at 350 °C for 50 sec. Finally, AuGe/Au was evaporated on the backside of the wafer to form the collector contact. The total device length was about 190 μm.

Figure 1 shows a schematic diagram of the DHBT single-waveguide structure carrier-injected optical intensity modulator, and the basic operation principle of the given device is as follows; when the carriers are injected into the base (waveguide) region of the transistor, the absorption coefficient in this region changes primarily due to the band-filling effect and the plasma dispersion effect, and hence, the output light intensity can be modulated. By reverse-biasing the base-collector junction, the injected carriers can be removed at a faster rate thereby reducing the optical switching speeds as compared to the diode-structured devices [5].

3. Measurements and Results

A schematic experimental set-up used for the determination of optical modulation characteristics is as shown in Fig. 2. A TE-mode output from an 869 nm GaAs DFB laser diode was end-fired coupled into the cleaved end face of the waveguide by a microscope objective (20×, NA 0.40). To permit the observation of the mode structure, the near-field pattern of the output was magnified with another microscope lens (20×, NA 0.40), and then imaged into an infrared vidicon and displayed on a TV monitor. The output power was also monitored using a Si photodiode. The transistor was operated in the common-emitter configuration, and the collector was reverse-biased at 1.5 V.

Figure 3 shows the relative change of the output light intensity measured at different levels of carrier injection. Also shown in Fig. 4 is the measured response trace of the light output to the injected emitter current. The spontaneous emission due to current injection was measured to be negligibly small compared to the beam power, which meant that the carrier lifetime in the base/waveguide region was determined mainly by the non-radiative recombination lifetime. It can be observed from Figs. 3 and 4 that the output light intensity *increases* almost linearly with the injection current, and up to 43% optical modulation has been obtained at a pulsed emitter current of $I_e \approx 100$ mA. The total insertion loss was about 23.4 dB. Assuming $m = \exp[-\Delta\alpha\,\Gamma L]$ dependence, where m is the on/off ratio of the optical powers after and before the current injection, $\Delta\alpha$ is the currentinduced absorption change, Γ is the overlap integral between the optical and current fields, and L is the device length, then $\Delta\alpha$ was approximately $-$ 20 cm^{-1} at $I_e \approx 100$ mA.

Presently, although the optical confinement factor of the waveguide is expected to be almost unity, Γ itself is thought to be somewhat small as indicated by the relatively poor values of the current gain h_{FE} of the transistor, a measured characteristics of which is as shown in Fig. 5. The h_{FE} was typically around 5, but the values varied in a range of 2~10 from device to device prepared on the same wafer. The reasons why h_{FE} values were small were primarily because of large surface recombination losses in the external base region, and an "energy-band spike" existing at the abrupt base-collector heterojunction interface, which prevented an efficient collection of carriers [7]. In fact, grading the base-collector heterojunction has improved the d.c. transistor performance [8], which in turn is expected to improve the overlap integral Γ and hence, the modulation on/off ratio m of the present device. Further improvements in the modulation on/off ratio can be expected, if the wavelength of the light source were chosen to be even closer to the band-edge wavelength λ_g. This is because the variations in the absorption coefficient and also the refractive index are much larger in this wavelength region.

The switching time t_r of the transistor was determined using the measured data of each resistance and the estimated values of each capacitance; load resistance $R_L = 50\ \Omega$, emitter resistance $R_e = 44\ \Omega$, base resistance $R_b = 24\ \Omega$, collector resistance $R_c = 0.1\ \Omega$, base-emitter depletion capacitance $C_{be} = 2.4$ pF, and base-collector depletion capacitance $C_{bc} = 4.9$ pF (at -1.5 V). A charge-control analysis yields [9],

$$t_r \approx \left[\tau_T h_{FE} + (R_e + R_b + R_L) C_{bc}\right] \times \ln\left(\frac{1}{1 - 0.9 I_c / I_b h_{FE}}\right)$$

where τ_T is the base transit time.

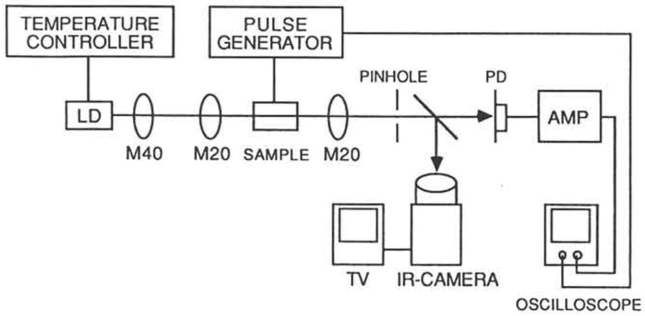

Fig. 2 A schematic set-up used for the determination of optical modulation characteristics.

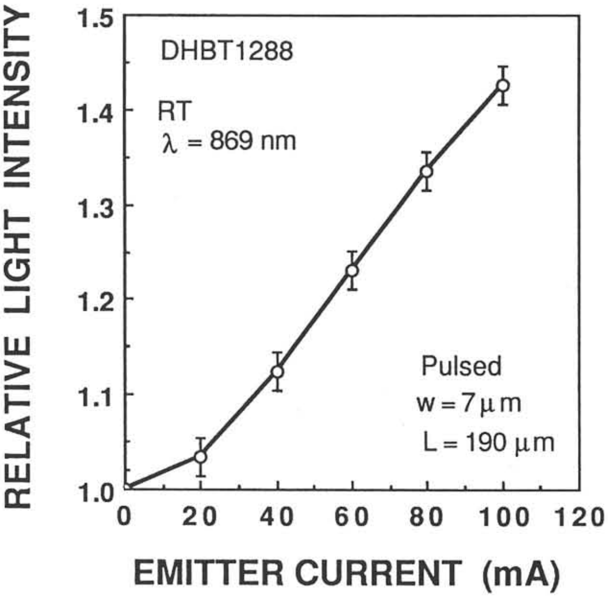

Fig. 3 Measured optical modulation characteristics.

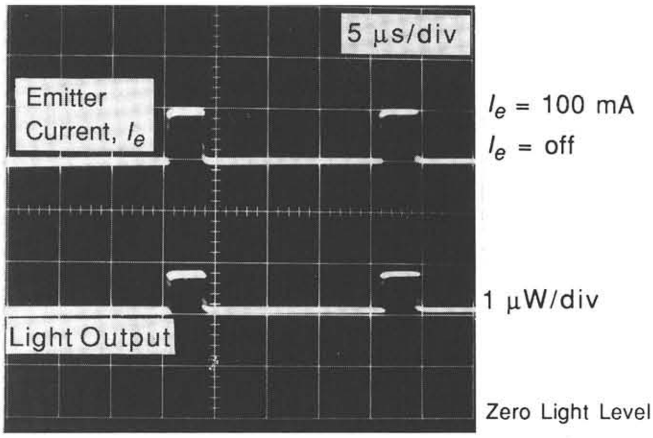

Fig. 4 Measured response of the light output to the injected emitter current.